The Role of Acidic Amino Acid Residues in the Structural Stability of Snake Cardiotoxins†

Chien-Min Chiang, Shou-Lin Chang, Hai-jui Lin, and Wen-guey Wu*

Department of Life Sciences, National Tsing Hua University, Hsinchu, Taiwan 30043

Received January 16, 1996; Revised Manuscript Received May 9, 1996⊗

ABSTRACT: We have recently shown that membrane-related activities of cardiotoxin V from *Naja naja atra* (CTX A5) are diminished at acidic pH although the overall β-sheet structure of the molecule is maintained. In order to understand more about the mechanism of inactivation of CTX at acidic pH, we studied the effect of pH and denaturing reagents on the structural stability of CTX. We found, first, pH-induced structural transitions occurred in CTX A5 at two pH values as judged by the CD ellipticity around 195 nm: an increase in the β-sheet content occurred around pH 4 and followed by a decrease, therein, around pH 2. The pK_a of three acidic amino acid residues in CTX A5, i.e., Glu-17, Asp-42, and Asp-59, were determined to be 4.0, 3.2, and below 2.3, respectively, by NMR spectroscopy. The low pK_a value of Asp-59 implies salt bridge formation between Lys-2 and Asp-59. Thus, electrostatic interaction may stabilize the three loop structure in addition to the hydrogen bonds between N- and C-termini of CTX molecule. Second, 2,2,2-trifluoroethanol (TFE) and guanidinium chloride (GdmHCl) were found to induce α-helical and random coil formation, respectively, in CTX A5 and eight other β-sheet CTXs. Comparison of the relative potencies of TFE and GdmHCl to induce structural changes suggests that the amino acid residue located at position 17 plays a role in the structural stability. Specifically, CTXs containing negatively charged Glu-17 are least stable. It is suggested that Glu-17 may perturb the interaction between Lys-2 and Asp-59, and thus the overall stability of β-sheet, in the presence of denaturing reagent. In conclusion, the perturbed structural stability of CTXs may partially explain the lower activity CTX exhibits at acidic pH. A structural model to account for the unfolding and refolding of CTX molecules without the breaking of disulfide bonds is also proposed.

Cardiotoxins (CTXs)[1] from cobra snake venom are basic β-sheet polypeptides with a characteristic three-finger loop structure that is stabilized by four disulfide bonds (Chien et al., 1994; Dufton & Hider, 1991). Their three-dimensional structures have been determined both by X-ray (Bilwes et al., 1994; Rees et al., 1990; Sun et al., 1996) and by NMR (O'Connell et al., 1993; Singhal et al., 1993; Gilquin et al., 1993; Bhaskaran et al., 1994a,b; Jahnke et al., 1994). CTXs bind to membrane phospholipids, and a continuous hydrophobic patch flanked by positively charged lysine residues is suggested to be involved in this interaction (Chien et al., 1994; Dauplais et al., 1995). In addition, several indications suggest that acidic amino acid residues play a role in the structure and activity relationship of CTXs.

First, most acidic residues of CTX molecules, e.g., Glu-17, Asp-42, and Asp-59, are located in highly conserved regions, indicating possible structural and functional roles (Table 1 and Figure 1). These acidic amino acid residues are located in the core region of three-finger loops and thus fall on the opposite side of three loops which are thought to constitute the putative phospholipid binding sites. This strategic separation of acidic and basic residues causes the polarization of the CTX molecules (Sun et al., 1996). Interestingly, the surface electrostatic potential of phospholipase A_2, a major component of snake venom with a synergistic toxic effect with CTX, also exhibits significant sidedness, i.e., polarized distribution of acidic and basic amino acid residues (Scott et al., 1994). This implies an electrostatic interaction of CTX with either phospholipase A_2 (Hseu & Wu, 1995) or other membrane components.

Second, a correlation of the amino acid sequences of CTXs with their membrane activities reveals that CTXs containing glutamic acid at the 17 position exhibit higher lipid binding and membrane perturbing activities, including the aggregation/fusion of sphingomyelin vesicles (Chien et al., 1991, 1994). Also, acidic pH was found to diminish membrane-related activities of CTX A5 (Chiang et al., 1996). The inactivation detected between pH 5 and 7 was attributed mainly, but not solely, to the change in the effective charge content of CTX A5 at the membrane/water interface caused by protonation of His-4 around pH 6.0, while inactivation below pH 5 was attributed mainly to local conformational changes in CTX A5. Interestingly, the overall β-sheet structure of CTX A5, reflected by NOE constraints of ^{1}H NMR experiments, remains intact between pH 2.5 and 7.0 despite the complete inactivation of CTX-induced aggregation/fusion of sphingomyelin vesicles at pH 3.0.

In order to investigate the mechanism responsible for the inactivation of CTX at acidic pH, we studied the structural stability of CTX at low pH and under denaturation caused by guanidinium chloride (GdmHCl) or 2,2,2-trifluoroethanol

† This work was supported by the National Science Council, Taiwan (Grants NSC 83-0208-M007-086; 84-2113-M007-015; 85-2113-M007-035Y).

* To whom correspondence should be addressed (Fax: 886-35-715934).

⊗ Abstract published in *Advance ACS Abstracts,* July 1, 1996.

[1] Abbreviations: CTX: cardiotoxin; TFE: 2,2,2-trifluoroethanol; CD: circular dichroism; NMR: nuclear magnetic resonance; NOE: nuclear Overhauser effect; TOCSY: total correlation spectroscopy; NOESY: nuclear Overhauser effect spectroscopy, GdmHCl: guanidinium chloride; DTT: dithiothreitol.

S0006-2960(96)00077-3 CCC: $12.00

Table 1: Relationship of the Amino Acid Sequences with the Structural Stabilities of CTXs As Probed by the Relative Potencies of TFE and GdmHCl To Induce Conformational Changes

CTX	Amino acid sequences	Structural stability*	
		TFE (%)	GdmHCl (M)
M4	LKC-NRLIPP FWKTCP<u>E</u>GKN LCYKMTMRLA P-KVPVKRGC IDVCPKSSLL IKYMCCNTNK CN	33	3.1
A5	LKCHNTQLPF IYKTCP<u>E</u>GKN LCFKATLKKF PLKFPVKRGC ADNCPKNSAL LKYVCCSTDK CN	42	3.2
M3	LKC-NKLIPI AYKTCP<u>E</u>GKN LCYKMMLASK -KMVPVKRGC INVCPKNSAL VKYVCCSTDR CN	64	3.8
M2	LKC-NQLIPP FWKTCP<u>K</u>GKN LCYKMTMRGA -SKVPVKRGC IDVCPKSSLL IKYMCCNTDK CN	75	4.2
M1	LKC-NQLIPP FWKTCP<u>K</u>GKN LCYKMTMRAA P-MVPVKRGC IDVCPKSSLL IKYMCCNTNK CN	80	4.5
A4	RKC-NKLVPL FYKTCP<u>A</u>GKN LCYKMFMVSN -LTVPVKRGC IDVCPKNSAL VKYVCCNTDR CN	85	4.5
A2	LKC-NKLVPL FYKTCP<u>A</u>GKN LCYKMFMVSN -LTVPVKRGC IDVCPKNSAL VKYVCCNTDR CN	86	5.0
A1	LKC-NKLIPI ASKTCP<u>A</u>GKN LCYKMFMMSD -LTIPVKRGC IDVCPKSNLL VKYVCCNTDR CN	88	4.5
A3	LKC-NKLVPL FYKTCP<u>A</u>GKN LCYKMFMVAT P-KVPVKRGC IDVCPKSSLL VKYVCCNTDR CN	88	4.5

*High stability of CTX molecule is reflected by the high concentration of the denaturing reagents required to induce 50% of the detected conformational change. The possible deviations of the data are estimated to be about 10%.

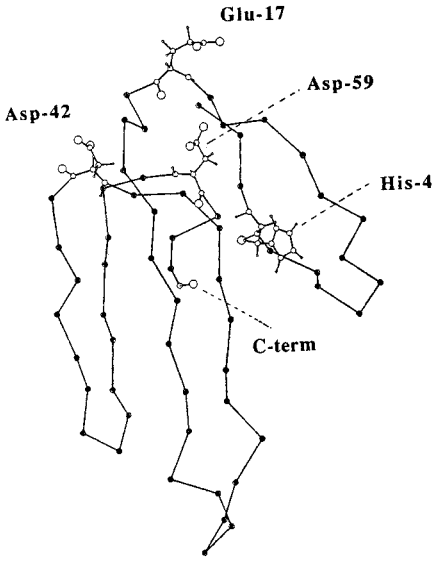

FIGURE 1: 3D solution structure of CTX A5 (CTX V from *Naja naja atra*) determined by NMR highlighting the titrable amino acid residues at acidic pH.

(TFE). It has been shown that decrease in cytotoxicity of toxin γ, a cardiotoxin from *Naja nigricollis*, may correlate with its structural stability (Roumestand et al., 1994). TFE and GdmHCl induce α-helix and random coil formation, respectively, in the all β-sheet CTXs (Galat et al., 1985; Roumestand et al., 1994). Therefore, comparative studies of the relative structural stability of CTX homologues may help delineate the amino acids responsible for the stability of CTXs. The effect of acidic pH on the structure and dynamics of CTXs, as monitored by change in CD ellipticity at different pH and by surveying the ^{1}H NMR chemical shift data available for 6 CTX homologues at different pH values (the present work; Otting et al., 1987; O'Connell et al., 1993; Singhal et al., 1993; Gilquin et al., 1993; Bhaskaran et al., 1994a; Jahnke et al., 1994), is described herein. As a result of this chemical shifts analysis, we suggest that the hydrogen bonds and salt bridge between N- and C-termini are an important stabilizing factor that help maintain the characteristic CTX structure with three-finger loops. A preliminary account of this structural transition has been presented elsewhere (Chiang et al., 1995).

MATERIALS AND METHODS

CTXs were purified from crude snake venoms of *Naja naja atra* and *Naja mossambica mossambica* (from Sigma Chemicals, St. Louis, MO) by SP-Sephadex C-25 ion exchange column chromatography and HPLC as described before (Chien et al., 1994). All other chemical reagents were reagent grade and obtained from Sigma or Merck.

Proton NMR Spectroscopy. ^{1}H NMR spectra were recorded at 25 °C on a Bruker DMX-600 spectrometer as described previously (Chiang et al., 1996). Briefly, 4 mM CTX A5 in H_2O/D_2O (90/10 v/v) at five different pH, i.e., pH 2.5, 3.0, 3.5, 5.1, and 7.0, was used. Before the desired pH was reached, a stepwise pH titration, about 0.1 pH unit, of the sample was carried out and routine one-dimensional ^{1}H NMR spectra were obtained at each step. TOCSY (Bax & Davis, 1985) with a mixing time of 55 ms and NOESY (Jeener et al., 1979; Macura & Ernst, 1980; Anil-Kumar et al., 1980) with a mixing time of 250 ms were recorded in the phase-sensitive mode using time-proportional phase incrementation (Marion & Wüthrich, 1983). Water suppression was achieved by pulsed field gradient method (Piotto et al., 1992). The chemical shifts were reference to HOD at 4.8 ppm.

For the reassignment of ^{1}H resonances of CTX A3 (Bhaskaran et al., 1994a), 10 mM protein dissolved in 5 mM phosphate buffer in H_2O/D_2O (90/10 v/v) at pH 4.0 was used (Chang, 1992). The sample appeared to be clear; no signs of aggregation were apparent. TOCSY with a mixing time of 90 ms and NOESY with a mixing time of 120 ms were recorded at 37 °C. The 2D spectra obtained at pH 4.0 are similar to those obtained at pH 3.0 (Yu, personal communication). The H_N and H_α chemical shift values reported in Table 2 are based on the spectra obtained at pH 3.0, kindly provided by Dr. Yu.

H_N and H_α NMR chemical shift values of six CTX homologues were obtained from previous reports (Otting et al., 1987; O'Connell et al., 1993; Singhal et al., 1993; Gilquin et al., 1993; Bhaskaran et al., 1994a; Jahnke et al., 1994) and the present work. Chemical shift comparisons were then carried out by calculating the standard deviation $[\Sigma_i(\delta_i - \delta)^2/n]^{1/2}$, where δ is the average of i known resonances.

Circular Dichroism Measurements. The pH- and denaturants-induced structural changes in CTXs were analyzed by CD spectroscopy at 25 °C. For pH-dependent studies, typically, 20 μM CTX in 2 mM citric acid buffer at desired pH was used. Citric acid has three pK_as of 6.4, 4.76, and 3.14 and therefore was used as a buffer. The spectra or signals at desired wavelength were recorded on either an AVIV 62A DS spectropolarimeter (Lakewood, NJ) or a Jasco J-500 spectropolarimeter. Both spectrometers were calibrated between 180 and 320 nm by using 1 mg/mL ammonium *d*-10-camphorsulfonate in a 1 mm cell, which shows a positive CD peak with an intensity of ~31.7 mdeg at 290.5 nm and a negative peak at 192.5 nm with a $I_{192.5}/I_{290.5}$ value within the range from 1.9 to 2.2. Similar signal intensities were generally obtained from the two spectrometers. CD spectra were routinely obtained using a bandwidth of 1 nm, a time constant of 1 s, and a 1 mm path length cell. CD spectra were the average of 8 repeats. The effect of GdmHCl on CTXs was reported as a fraction of CTX unfolded calculated from CD signals at 212 nm. TFE-induced α-helix formation was measured from CD signals at 222 nm. All CD data are reported as mean residue ellipticity.

For the comparative stability experiments of CTX homologues, 20 μM protein in 20 mM phosphate buffer (pH 7.4) containing different GdmHCl concentrations was used. TFE-induced structural change was determined using 20 μM CTX in different TFE/H_2O mixtures in the absence of buffer as a buffered solution turned turbid at high concentration of TFE. To prepare a sample with the same CTX concentration in different GdmHCl or TFE solutions, aliquots (9 nmol) of concentrated CTX were transferred to different vials and lyophilized to dryness and then reconstituted with a 450 μL solution containing the desired concentration of denaturing reagent.

Ellman Assay for Thiols. In order to check the integrity of the four disulfide bonds, the Ellman assay was carried out for determination of free thiol content of CTX in both the TFE/H_2O mixture and the GdmHCl containing solution. The absorbance at 412 nm was monitored with dithiothreitol (DTT) as control (Ellman, 1959; Riddles et al., 1983).

RESULTS

NMR and CD Studies of the Effect of Acidic pH on CTX A5

Determination of pK_a of Acidic Amino Acid Residues. In our previous study, the pK_a of His-4 was determined to be about 5.6 (Chiang et al., 1996). In the present study, we use the same sequential assignment information obtained from TOCSY and NOESY 2D NMR spectra at pH 2.5, 3.0, 3.5, 5.1, and 7.0 to identify ^{1}H resonances in 1D spectra recorded at approximately each 0.1 pH unit. In order to determine the exact pK_a values, pH-dependent ^{1}H NMR chemical shifts were fitted according to Hill equation for a one-proton titration process.

It should be pointed out that previous ^{1}H NMR studies of CTXs from *N. m. mossambica* reveal large pH-dependent shifts in amide proton resonances for both the titrable residues and their neighboring amino acid (Lauterwein et al., 1978; Steinmetz et al., 1981, 1988). For instance, chemical shifts of the amide protons of Asp-42 and Val-43 of CTX M2 were found to vary with pH, which is interpreted to be a result of titration of the carboxylate group of Asp-42 whose pK_a value is 2.6 (Steinmetz et al., 1988).[2] Interestingly, the chemical shifts of δ-methyl protons of Ile-41 were also found to exhibit similar titration shift with the same apparent pK_a of 2.6. Since the methyl protons are relatively inert and are lost only to reagents as strong as *tert*-butyllithium, these shifts strongly suggest that a pH-induced local conformational change indeed occurs near the titrable carboxyl group of Asp-42. These results suggest, furthermore, under suitable conditions that the pH-dependent behavior of amide proton of the main chain may serve as a useful probe in determining the pK_a values of the side chain carboxyl groups of acidic residues in CTXs.

Usually the chemical shifts of the adjacent ^{1}H or ^{13}C are followed for measurement of the side chain pK_a values (Kohda et al., 1991; Jeng & Dyson, 1996). Unambiguous assignments of pK_as for most of the ionized groups of human thioredoxin could not be made based only on the amide proton shifts due to complexity of interaction involved (Forman-Kay et al., 1992). Nevertheless, amide proton shifts of bull seminal inhibitor IIa in H_2O have enabled characterization of the pK_a values of most of the carboxyl groups in the protein (Ebina & Wüthrich, 1984). We therefore felt it worthwhile to see if the variation in H_N chemical shift with pH would reflect pK_a values of the side chains of CTXs like the values determined by the adjacent ^{1}H shifts.

Shown in Figure 2 is the pH titration dependence of chemical shifts of the amide protons and protons adjacent to the carboxyl group, i.e., γ-CH2 of Glu-17 and β-CH2 of Asp-42. They showed apparent pK_a values of 4.0 and 3.2, respectively. The intrinsic pK_a values of ionizable carboxyl groups of side chains of Glu and Asp have been reported to be 4.3 and 3.9, respectively (Creighton, 1993). The slightly lower pK_a values of the two aforementioned amino acid side chains may be due to the lowering of proton concentration near the polypeptide surface by the 12 positively charged Lys or Arg side chains present in CTX A5. It can be concluded that the side chain carboxyl groups of both Glu-17 and Asp-42 are fully exposed to solvent.

It should be pointed out that there is no significant change in the chemical shift of amide proton of Asp-59 within the studied pH range between pH 2.3 and 7.0. The sensitivity of the amide proton chemical shifts to the protonation state of its side chain (Steinmetz et al., 1981, 1988) suggests that the pK_a of the side chain of Asp-59 is lower than the lowest studied pH of 2.3. This is consistent with the observation that the side chains of Lys-2 at the N-terminal and Asp-59 at the C-terminal form a stable bidentate salt bridge, as found in the X-ray crystal structure of CTX A5 determined at pH 6.8 (Sun et al., 1996). In fact, neighbors of amino acid residues 2 and 59 in CTXs showed interresidual NOE connectivities in all reported NMR studies. Since the conserved Lys-2 and its positive side chain lie near the negatively charged Asp-59, electrostatic interaction between Asp-59 and Lys-2 may very likely provide an additional stabilizing force to hold the two termini in close proximity. As will be shown later, the β-sheet structure of CTX A5 unfolds at pH below 2.3, supporting this conclusion.

[2] Note: We use A and M to represent the origin of snake venom from *Naja naja Atra* and *Naja mossambica Mossambica*, respectively. Please refer to Table 1 for the nomenclature and amino acid sequence numbering of the designated CTXs used in this study.

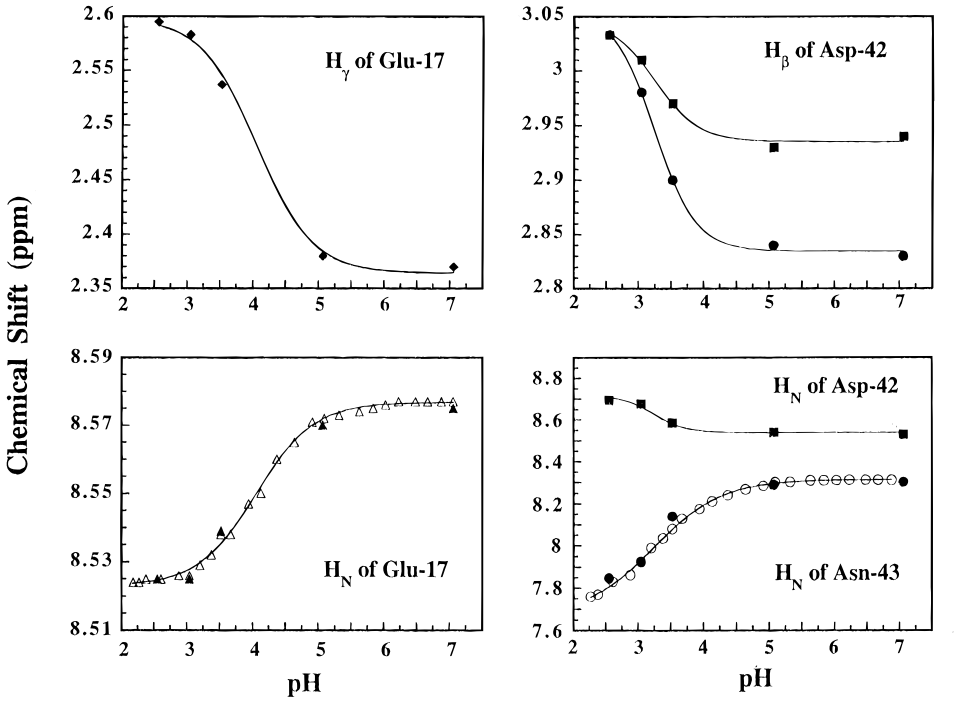

FIGURE 2: pH-dependent profile of the chemical shifts of proton resonances used to determine the pK_as of the ionizable group Glu-17 and Asp-42. Data sets represented by closed and open symbols are obtained from 2D and 1D NMR experiments, respectively. Solid lines are simulated curves using the pK_a value of 4.0 (left panels) and 3.2 (right panels).

pH-Induced Structural Transition of CTX A5. We have previously reported one pH-induced structural change of CTX A5 indicated by the CD intensity measurement at 205 nm between pH 2.9 and 7.0 (Chiang et al., 1996). We found that structural changes in CTX A5 occur at least at two pH ranges (Figure 3A,C), by monitoring the CD band near 195 nm, the wavelength indicative of the β-sheet content, and by studying the effect of low pH. Apparent stabilization of the β-sheet structure was found to occur when the pH was lowered from 5 to 2.5 and destabilization, from 2.3 to 1. Stabilization may have occurred due mainly to the protonation/deprotonation of either Glu-17 or Asp-42 or both, since pK_as of these two acidic amino acids are 4.0 and 3.2, respectively. The denaturation of CTX A5 below pH 2.3 could only have occurred due to the protonation process of the carboxyl groups from Asp-59 and/or C-terminal. It should be emphasized that, although the CD spectra exhibited marked difference, the NMR NOE connectivities of CTX A5 have been found to exhibit characteristic β-sheet structure through the pH range 2.5−7.0 (Chiang et al., 1996).

In order to determine which residue, Glu-17 or Asp-42, is involved in the apparent stabilization upon protonation, we performed similar pH titration on CTX A3, which contains Asp-42 but, instead of Glu-17, contains Ala-17 (see Table 1).

Comparative Studies of CTX Homologues

pH-Induced Structural Transition of CTX A3. As shown in Figure 3B, CTX A3 exhibits a characteristic CD spectrum of β-sheet structure: a high positive band at 195 nm and a much weaker negative band at 214 nm (Greenfield & Fasman, 1969). CTX A3 thus represents more characteristic β-sheet structure than CTX A5, despite the overall similarity of their three-dimensional solution structures based on NMR NOE connectivities. Shown in Figure 3C is the titration study of CTX A3. Two titrable regions, one above and one

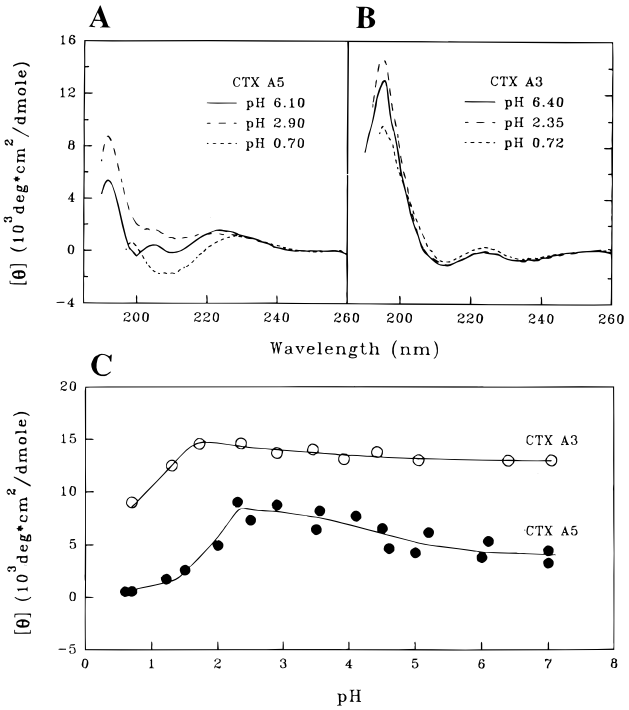

FIGURE 3: pH-induced structural changes of CTX A5 and CTX A3 as determined by CD spectroscopic study: representative CD spectra of CTX A5 (panel A) and CTX A3 (panel B) at the indicated pH; CD peak intensity around 195 nm as a function of pH (panel C). Solid lines in panel C are least-squares-fitted curves with apprant pK_a value of 2.6 and 4.2 for CTX A3 at pH above 2 and CTX A5 at pH above 3, respectively.

below pH 2.0, are evident. Like that for CTX A5, significant destabilization of the β-sheet structure in CTX A3 was found to occur below pH 2.0. In view of the structural similarity between CTX A3 and A5 near the C-terminal (Figures 4 and 5), the structural transition assigned reflects conformational change upon protonation of Asp-59. The small, but

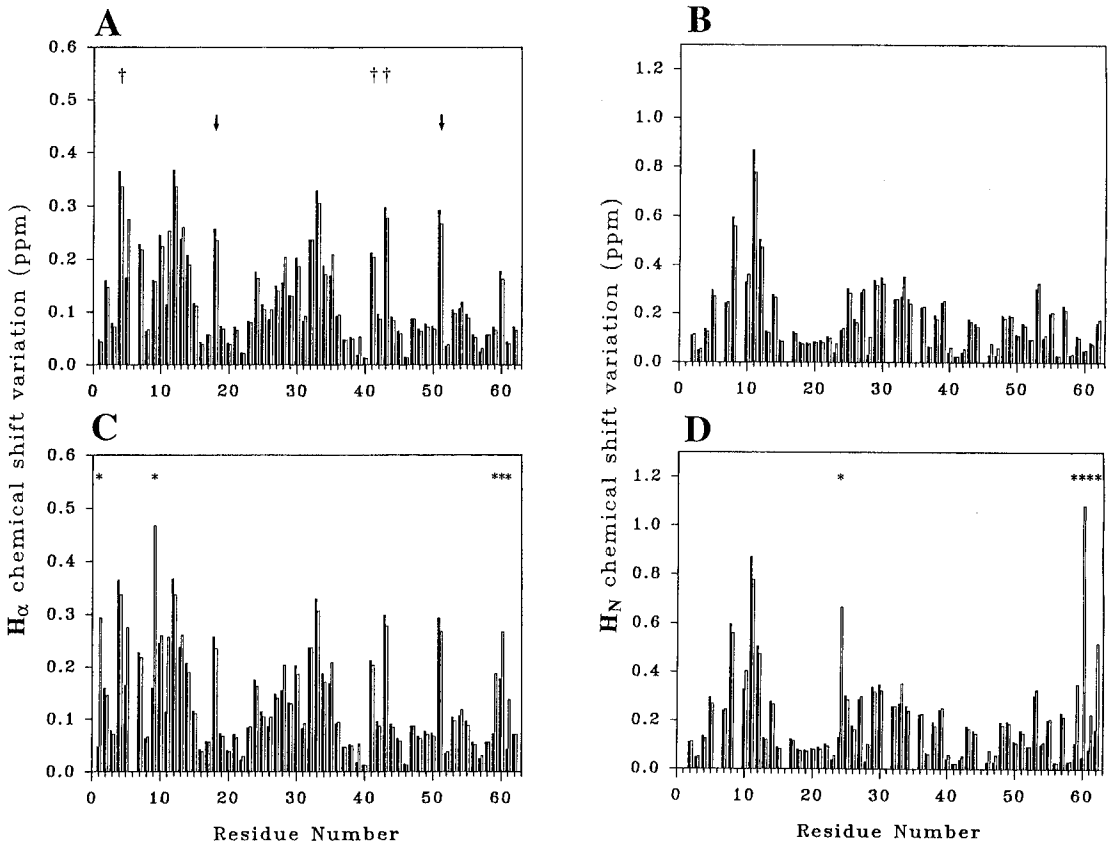

FIGURE 4: Comparison study of the chemical shifts variation of H_α (panels A and C) and H_N (panels B and D) of six CTX homologues. To indicate structural differences, the standard deviation $[\Sigma_i(\delta_i - \delta)^2/n]^{1/2}$, where δ is the average of i known resonances, was used to calculate the variations. Filled bars denote the variations of five CTXs (CTX A1, A5, M1, M2, toxin γ), and open bars denote variations for all six CTXs (including CTX A3). Chemical shifts of CTX A3 reported previously (panels C and D) and our newly assigned values (panels A and B) are used to enable direct comparison. Large variations in the chemical shifts of conserved residues are indicated by "†" and "↓" in panel A (see Table 1 and text for details). The chemical shift variations including CTX A3 (panels C and D, open bars) clearly stand out as deviating markedly from those excluding CTX A3 (panels C and D, filled bars), as denoted by "*". Please note that the alignments of the amino acid sequences from 4 to 6 positions are shifted forward by one amino acid residue as compared with Table 1. We shift the position in this comparison because the NOE connectivities establishing the β-sheet structure in the loop I region are continuous from residues 1 to 5 in all reported CTX structures.

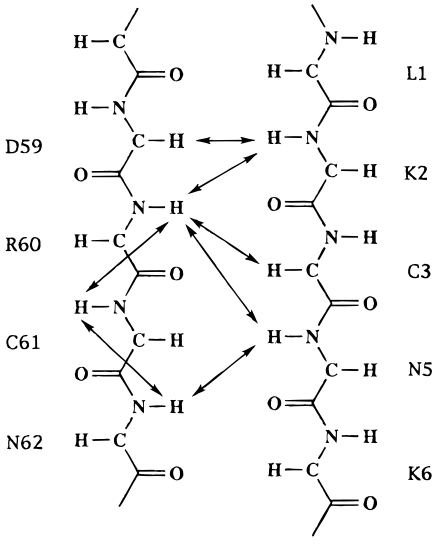

FIGURE 5: Schematic diagram of the NMR NOE connectivities involving the N- and C-termini of CTX A3. A similar profile is obtained for the sample studied at pH 3.0 and 4.0. Similar NOE connectivities have also been observed for CTX A5 between pH 7 and 2.5 (Chiang et al., 1996).

detectable, stabilization effect on β-sheet structure of CTX A3 between pH 5 and 2 can then be attributed to Asp-42. We therefore conclude that both Asp-42 and Glu-17 contribute to the structural transition of CTX A5 between pH 5 and 2.5. Glu-17 is judged to contribute more significantly, though, judging by the relative change in CD intensity of CTX A3 and A5.

Denaturation of CTX A3 occurs below pH 2.0. Asp-59 resists protonation in the normal pH range and therefore must be involved in interacting with other positively charged amino acid residues near the C-terminal. In the following section, we compare the available chemical shifts of CTXs to further illustrate this point.

Structural Similarity of CTX Homologues near the C-Terminal as Revealed by Chemical Shift Analysis. In order to determine whether the interaction between N- and C-termini occurs in other CTXs, we compared the chemical shifts of CTXs whose structures were determined at different pH (Otting et al., 1987; O'Connell et al., 1993; Singhal et al., 1993; Gilquin et al., 1993; Bhaskaran et al., 1994a; Jahnke et al., 1994). Although the three-dimensional structures determined by X-ray diffraction and NMR NOE constraints have revealed structural similarity and close proximity of the N- and C-termini, we felt it is important to examine details of interaction by the NMR chemical shifts, a more sensitive parameter, for comparison of structural stability of different CTXs. For instance, previous 2D NMR and CD spectroscopic studies of mouse epidermal growth factor (Kohda et al., 1991) have detected conformational

changes, in pH titration experiment, with CD and NMR chemical shift, but they failed to detect similar conformational change by semiquantitative interpretation of NOEs. We therefore analyzed the amide and C_α proton chemical shift variations in order that the structural region related to stability may stand out (Pardi et al., 1983; Wishart et al., 1992).

The results as obtained from the data of CTX A1, A5, M1, M2, and toxin γ (Figure 4, filled bars) indicate that their 3D structures differ mainly near the tips of loops I and II. For instance, the H_N chemical shift variations, determined by the standard deviation of the five CTXs compared, indicate that maximum deviation is centered at amino acid positions 11 and 30 (Figure 4B). This is consistent with the observation that both the primary sequence and local conformation in these regions of the CTXs studied are significantly different (Chien et al., 1994).

Three regions with H_N chemical shift variation lower than 0.2 ppm can be identified in N-terminal and C-terminal and around amino acids between 15 and 23. As discussed later, these three regions are proposed to be responsible for the pH- and denaturant-induced structural transition of CTXs. Specifically, the interactions among Lys-2, Asp-59, and Glu-17, which is also proximal to the putative salt bridge between side chains of Lys-2 and Asp-59, may explain the relative structural stability observed in this study of CTX homologues. Also, chemical shifts for the amino acids 40−47 do not vary significantly. Nevertheless, these amino acid residues are conserved (Table 1) and have been detected to be involved in dimer formation at least in the X-ray structures of CTX A5 and M3 determined near physiological pH (Rees et al., 1993; Sun et al., 1996).

Similar conclusion can also be made by comparison of H_α chemical shift variations, but there are several interesting exceptions (Figure 4A). For instance, the H_α chemical shifts of the conserved Gly-18 are found to vary significantly. Significant variation is also found at position 51 where conserved hydrophobic residues Val, Iso, or Leu are located (Wüthrich, 1986). Interestingly, both residues 18 and 51 lie in the turn region. Other exceptions arise mainly due to the deviations in resonances of residues 4, 41, and 43 of CTX A5. These variations probably arise due to the ring current effect of His-4 and to the difference in amino acids, the Ala-41 and Asn-43 (see Table 1), in CTX A5. Above all, with the exception of H_α resonances of position 18 and 51, emphasized by the arrows, chemical shift variations from both H_α and H_N (Figure 4A,B) can be understood to be a result of the conformational differences near the tip of loops I and II.

Reassignment of ^{1}H NMR Signals of CTX A3 and Comparison with Other CTXs. As a spinoff of chemical shift analyses, resonance assignments for CTX A3 reported previously (Bhaskaran et al., 1994a) are found to be erroneous, or to at least deserve further investigation, if these data are to be used for future studies. The new assignments of several H_N and H_α resonances of CTX A3 are listed in Table 2. The NOE connectivities involving the amino acid residues of the C-terminal, depicted in Figure 5, are based on the new assignments. Chemical shift variations of both H_N and H_α were also compared by including the data of CTX A3 (Figure 4, open bars) using either our newly assigned (panels A and B) or previous (panels C and D) NMR assignments. As emphasized by the star symbol shown in Figure 4C,D, previous assignments at the indicated positions introduce marked effect in increasing the chemical shift variation of H_N or H_α or both. In addition, the NOE through-space connectivities between H_α/Tyr-23 and H_N/Lys-24, H_N/Lys-24 and H_α/Cys-55, H_N/Asn-5 and H_N/Asn-62, H_N/Lys-2 and H_N/Arg-60, H_N/Asn-5 and H_α/Arg-60, and H_N/Leu-10 and H_N/Phe-11 are all missing in previous assignments. These connectivies are present in all published CTX structures and should also be detectable in CTX A3 in its reported 3D structure (Bhaskaran et al., 1994a). It should be noted that the amino acid numbering used here, shown in Table 1, is different from that used previously. We point out that the NMR assignments of CTX A2 and neurotoxin from *N. n. atra* (Bhaskaran et al., 1994b; Yu et al., 1990, 1993) probably need further investigation based on similar reason.

Table 2: The Reassigned Values of ^{1}H Chemical Shifts of CTX A3 (CTX III from *Naja naja atra*) in 10% D_2O/H_2O at pH 3.0, 20 °C

	chemical shift (ppm)[a]	
residue[2]	H_N	H_α
Leu-1		4.20
Pro-9		4.56
Leu-10	6.73	4.48
Phe-11	8.16	4.86
Lys-24	9.07	4.93
Asp-59	8.21	4.87
Arg-60	9.69	3.42
Cys-61	7.58	4.49
Asn-62	9.16	4.41

[a] The reported chemical shifts were measured relative to 4,4-dimethyl-4-silapentane-1-sulfonate. Please refer to Bhaskaran et al. (1994a) for the assignment of other resonances. Based on these reassignments of H_N and H_α, their respective side chain proton resonances need to be reinvestigated.

Comparison of the H_N and H_α chemical shifts of six CTXs (CTX A1, A3, A5, M1, M2, and toxin γ) using the newly assigned resonances indicates that the structures of all CTXs near the C-terminal are similar (Figure 5). In addition, at least for CTX A3 and A5, the pK_a of Asp-59 is well below pH 3.0 as judged from the pH-dependent NMR chemical shift and CD intensity study of CTX A3 and A5 (Figure 3).

The low pK_a of Asp-59 in CTXs suggests that the positively charged ϵ-ammonium group of Lys-2 is very proximal to the titrable β-carboxyl group of Asp-59. The electrostatic interaction between the two groups can provide an additional stabilizing factor for most, if not all, CTX homologues. It should be emphasized that the C- and N-terminal regions are connected by not only salt bridge but also the main chain hydrogen bonds such as those between H_N of Lys-60 and CO of Lys-2 (Figure 5). These main chain hydrogen bonds have also been reported to be present in all CTX structures determined either by NMR or by X-ray. Hydrogen bonds involving other side chains in this region probably contribute to the stabilization of C-terminal.

Structural Stability of CTXs As Revealed by TFE-Induced β-Sheet to α-Helix Transition. Shown in Figure 6 is the effect of TFE on the CD spectra of CTX A5. Characteristic CD signals representing α-helix structure with high negative ellipticity at 222 and 208 nm are clearly visible for TFE concentrations above 60%. Similar transition to α-helix of CTX A3 caused by 90% TFE was presented (Galat et al., 1985). We found, based on ellipticity at 222 and 208 nm, that about 30% amino acid residues in CTX A5 are involved in helix formation, but the molecular ellipticity of the band

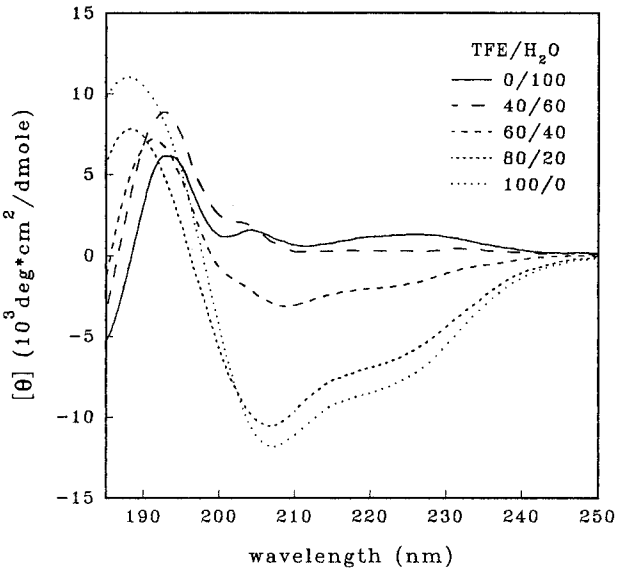

FIGURE 6: CD spectra of CTX A5 (mean residue ellipticity) at the indicated TFE/H_2O ratios.

near 195 nm was lower than expected from the α-helix contents estimated at 222 and 208 nm. This was suggested to be due to the formation of deformed α-helix under the geometric constraint of four disulfide bonds (Galat et al., 1985). All four disulfide bonds were found to remain intact during the β-sheet to α-helix transition as detected by Ellman assay (data not shown). The integrity of disulfide bonds is further supported by our observation that the studied transition reverses upon dilution of the TFE with water.

Unlike TFE-induced structural transitions of other proteins or polypeptides (see, for instance, Shiraki et al., 1995), a clear isosbestic point in CD spectra of CTX A5 is absent, as has been observed earlier for CTX A3 (Galat et al., 1985). This suggests that more than two conformational states of CTX in TFE/H_2O are present. In addition, the effect does not seem to be cooperative since only a modest change occurs over a large concentration range of TFE.

In order to understand the role of specific amino acids in the structural transition induced by TFE, we performed similar studies on various CTX homologues with known amino acid sequences. Figure 7A shows the effect of TFE on the structure of nine CTX homologues as detected by CD spectroscopy. The molecular ellipticity at 222 nm of the studied CTX homologues is similar, which suggests that the number of amino acid residues involved in the TFE-induced α-helix formation is similar. The relative potencies of TFE-induced structural changes of the CTXs studied are listed in Table 1.

Structural Stability of CTXs As Revealed by GdmHCl-Induced β-Sheet to Random Coil Transition. In order to determine whether the TFE-induced β-sheet to α-helix transition is due to the perturbed stability of CTX molecule or to the intrinsic tendency of CTX to form α-helix structure, we studied the GdmHCl-induced unfolding of β-sheet to random coil (Roumestand et al., 1994) for the nine CTX homologues. It has been suggested that alcohols such as TFE in water weaken the hydrophobic interaction and strengthen the helical propensity, whereas GdmHCl in water weakens both types of interactions (Thomas & Dill, 1993). As seen in Figure 7B, GdmHCl-induced unfolding of β-sheet to random coil depends on the types of CTXs, and thus their amino acid sequences.

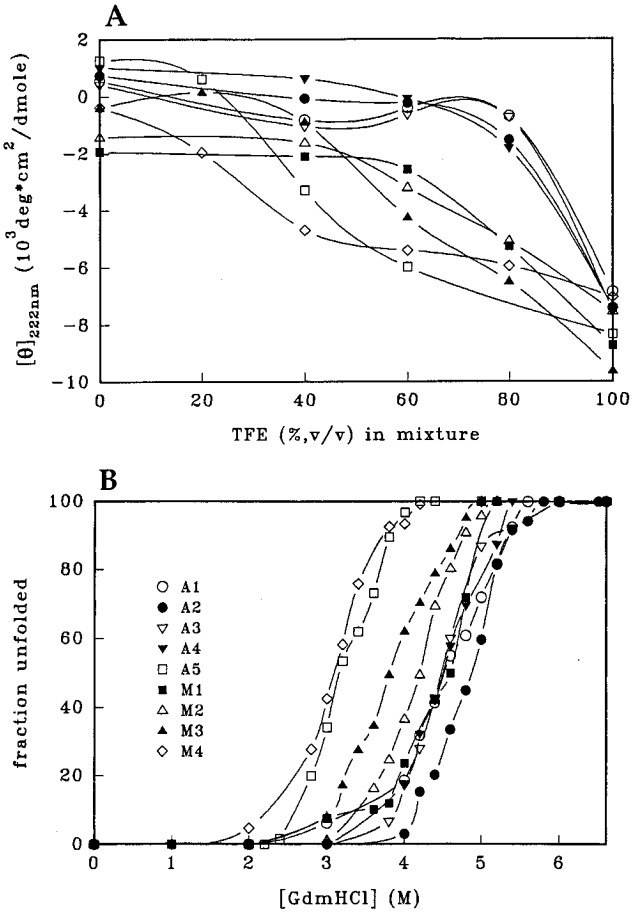

FIGURE 7: Comparative study of the structural stabilities of nine CTX homologues in the presence of TFE (panel A) and GdmHCl (panel B) by CD spectroscopy. The symbols in panel B indicate the respective CTX homologue and are common to both panels. The amino acid sequences of the indicated CTXs can be found in Table 1.

The concentration of GdmHCl needed to unfold 50% of the CTX molecules is listed in Table 1. Despite the observation that the two denaturing reagents induce different conformational changes, lower concentrations of both are required for CTX M4, A5, and M3 to induce 50% change. In fact, a good correlation can be found between the relative potency of GdmHCl- and TFE- induced structural transition of CTXs (Figure 8). Careful examination of the amino acid sequences shown in Table 1 reveals that amino acid residue at position 17 appears to be most relevant in the structural change. In general, Ala-17 containing CTXs appear to be more stable than Glu-17 containing CTXs.

DISCUSSION

The importance of residue 17 in the structural stability of CTXs was quite surprising. First, Glu-17 of CTX A5 is located at the base of the three-finger loops (Figure 1) and is fully exposed to water as indicated by its normal pK_a of about 4.0. Second, the overall three-dimensional β-sheet structure of CTX A5 does not undergo significant changes at different pH as evidenced by the NMR NOE connectivities and amide and C_α proton chemical shifts (Chiang et al., 1996; see also Figures 4 and 5). Most of the NMR chemical shift differences of the amide protons of CTX A5, for example, at different pH can be explained by the difference in protonation states of the imidazole ring of His-4 and side chain carboxyl groups of Glu-17 and Asp-42 (Chiang et al.,

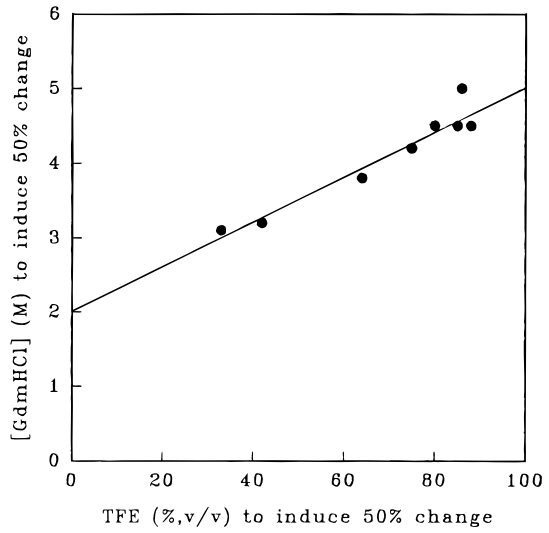

FIGURE 8: Correlation of the relative potency of TFE- and GdmHCl-induced structural transition of CTXs.

1996). Therefore, the perturbed structural stability, as revealed by TFE- and GdmHCl-induced structural changes of nine CTX homologues, may reflect electrostatic interactions involving mainly local amino acid residues.

It was also surprising to find that the four disulfide bonds of CTX were intact in spite of α-helix formation in the presence of TFE. TFE-induced α-helix formation in CTX A3 has previously been observed (Galat et al., 1985). It should be pointed out that in our studies the presumed β-sheet to random coil transition, followed by α-helix formation, occurs only at TFE concentrations higher than 50%. A careful examination of CD data reveals that, at TFE concentration below 40%, CTX A5 exhibits higher β-sheet content than its native state as evidenced by slightly higher CD ellipticity around 195 nm. Lipid-induced increase in the content of β-sheet at the expense of the nonordered conformation has previously been observed based on IR, CD, and NMR measurements (Surewicz et al., 1988; Chien et al., 1994; Dauplais et al. 1995). In this respect, the suggestion that the TFE/H_2O mixture can mimic phospholipid micellar environments (Briggs & Gierasch, 1984; Macquaire et al., 1992; Fan et al., 1993; Rizo et al., 1993; Blanco et al., 1994) may only be valid in CTX systems at low TFE concentrations.

TFE is known to stabilize an existing α-helix structure of most proteins or polypeptides (Nelson & Kallenbach, 1986; Segawa et al., 1991; Dyson et al., 1992a,b). In fact, all proteins are expected to form α-helix structure at high TFE concentration (Thomas & Dill, 1993). This has been observed for β-sheet proteins (Zhong and Johnson, 1992; Fan et al., 1992; Shiraki et al., 1995). Alcohols such as TFE act mainly by weakening the hydrophobic interactions (Thomas & Dill, 1993) and slightly enhancing local helical interactions (Nelson & Kallenbach, 1986). The effect of TFE on electrostatic interaction is believed to be small although it has been argued that the lower dielectric constant of TFE, 26.8 vs 78.5 of water at 25 °C (Llinás & Klein, 1975), may increase electrostatic interaction among polar amino acid residues.

Regardless of the details of the mechanism of the alcohol-induced denaturation, the effects of TFE have also been found to be strongly sequence-dependent (Segawa et al., 1991; Sönnichsen et al., 1992) and appear to correlate with the propensity of α-helix formation, if such a propensity exists (Shiraki et al., 1995). The strong correlation observed in this study between the GdmHCl- and TFE-induced effects (Figure 8), however, suggests that the structural stability of β-sheet, rather than the propensity of α-helix formation, dictates the TFE-induced structural transition of CTXs. In the following, we propose a model based on the electrostatic interaction and hydrogen bond formation between the C- and N-termini to account for the structural stability of CTXs.

As shown in the schematic diagram in Figure 9, CTX can unfold without disrupting the disulfide bonds. The major energy barrier for the unfolding process may be the main chain hydrogen bonds between loops II and III (Singhal et al., 1993), the hydrophobic interaction between the tips of the three loops (Chien et al., 1994; Sun et al., 1996), the salt bridge, and the hydrogen bonds between the C- and N-termini (Sun et al., 1996, and this study). Since the residue identified to be responsible for the structural stability is located at position 17, which is known to lie close to the C-terminal, our results suggest that the interaction between the C-terminal and N-terminal regions plays a crucial role

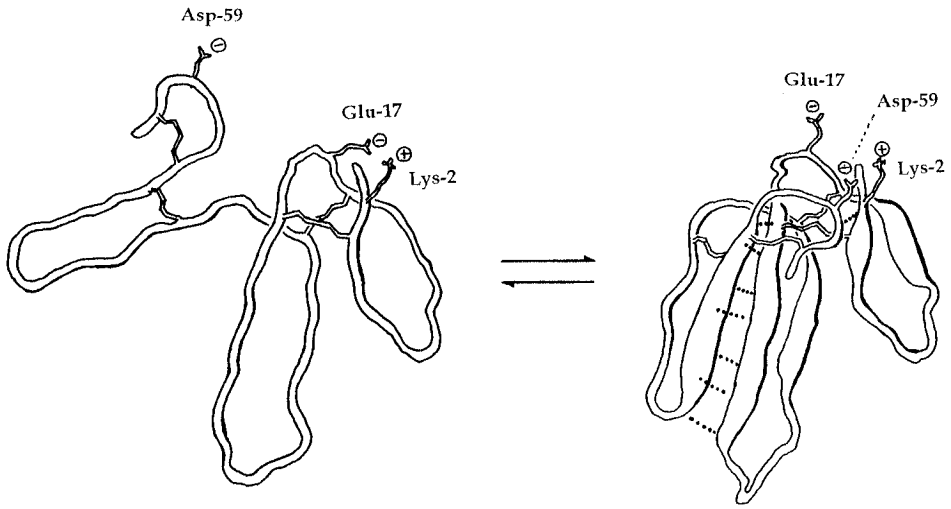

FIGURE 9: A hypothetical model explaining the unfolding of CTX molecules without the breakage of the four disulfide bonds. The main chain hydrogen bonds involved in unfolding are indicated by dots. The putative salt bridge between Asp-59 and Lys-2 in native β-sheet structure and the putative interaction between Glu-17 and Lys-2 in the unfolded state are also shown.

in the overall structural stability of CTX molecules. Gdm-HCl and TFE may thus act simply as denaturing agents and perturb significantly the hydrophobic interaction and hydrogen bond formation which are the major stabilization forces for maintaining the overall structure. The detection of other weaker stabilizing force such as the electrostatic interaction among Glu-17, Asp-59, and Lys-2 then becomes possible. We propose that Glu-17 may replace Asp-59 to interact with Lys-2 under favorable conditions. This model also explains the apparent stabilization caused by the protonation of Glu-17 and Asp-42 and the destabilization caused by the protonation of Asp-59 (or C-terminal carboxyl group).

The proposed model, although adequate to understand the structural stability of CTXs, may need further modification in the future. For instance, electrostatic attraction between Lys-2 and residue 17 may be insufficient to explain why CTXs containing Lys-17 are also less stable than those containing Ala-17. It has been pointed out earlier that the substitution of a Glu by a Lys may not be as simple as replacing a negative charge by a positive charge (Warshel & Aqvist, 1991; Cutler et al., 1989). In addition, it has been shown that changes in free energy of unfolding of single residue mutants with different charged residues are usually not additive because too many interactions change simultaneously (Serrano et al., 1990). Therefore, more precise determination of the side chain conformation under different experimental conditions is necessary to improve the model.

Dynamic perturbation of the phospholipid binding site has been found to correlate well with the toxicities of the chemical derivatives of toxin γ (Roumestand et al., 1994). Since the overall three-dimensional structure of CTX A5 at various pH and that of chemically modified toxin γ remain largely unperturbed, the study of the structure−function relationship of CTXs will probably have to rely on the detailed structural and dynamic analyses of CTX molecules. This can be done by analyzing more sensitive structural parameters such as NMR chemical shifts (Pardi et al., 1983; Williams, 1989; Wishart et al., 1992) obtained under different experimental conditions.

The structural stability of polypeptides is a reflection of the overall molecular interactions among all amino acid residues. For instance, the structural stability of CTX A5 can be considered to be "perturbed" at neutral to acidic pH although higher β-sheet content is detected. In contrast, a more pronounced and an entirely different perturbation of structural stability is detected by further lowering the pH from 2 to 1. Based on these observations, the inhibition of the membrane-related activity of CTX A5 at acidic pH may be explained by the perturbed structural stability of the molecule at acidic pH.

Future experiments using bacterially expressed mutants (Chi et al., 1994) would provide more conclusive information regarding the roles of specific amino acid residues in the structural stability of CTX molecules. It would also be interesting to determine how the membrane environment would perturb the structural stability of CTX molecules.

ACKNOWLEDGMENT

We thank Dr. H. W. Huang for his kind help for use of the CD spectrometer and useful discussions. We are also indebted to the Hsinchu regional research facility center for use of the Bruker DMX-600 NMR spectrometer. Suggestions of the unfolding model and help in NMR data processing from Drs. C. K. Hwang, P. C. Lyu, J. W. Cheng, and A. Warshel are also appreciated.

REFERENCES

Anil-Kumar, Ernst, R. R., & Wüthrich, K. (1980) *Biochem. Biophys. Res. Commun. 95*, 1−6.
Bax, A., & Davis, D. G. (1985) *J. Magn. Reson. 65*, 393−402.
Bhaskaran, R., Huang, C. C., Chang, D. K., & Yu, C. (1994a) *J. Mol. Biol. 235*, 1291−1301.
Bhaskaran, R., Huang, C.-C., Tsai, Y.-C., Jayaraman, G., Chang, D.-K., & Yu, C. (1994b) *J. Biol. Chem. 38*, 23500−23508.
Bilwes, A., Rees, B., Moras, D., Ménez, R., & Ménez, A. (1994) *J. Mol. Biol. 239*, 122−136.
Blanco, F. J., Jiménez, M. A., Rico, M., Santoro, J., & Nieto, J. L. (1993) *J. Am. Chem. Soc. 115*, 5887−5888.
Briggs, M. S., & Gierasch, L. M. (1984) *Biochemistry 23*, 3111−3114.
Brown, L. R., & Wüthrich, K. (1992) *J. Mol. Biol. 227*, 1118−1135.
Chang, S. L. (1992) High resolution NMR studies of CTX III from Taiwan cobra, M.S. Thesis, National Tsing Hua University.
Chi, L.-M., Vyas, A. A., Rule, G. S., & Wu. W. (1994) *Toxicon 32*, 1679−1683.
Chiang, C.-M., Huang, H. W., & Wu. W. (1995) *FASEB J. 9*, A1314.
Chiang, C.-M., Chien, K.-Y., Lin H.-j., Lin, J.-F., Yeh, H.-C., Ho, P., & Wu, W. (1996) *Biochemistry 35*, 9167−9176.
Chien, K.-Y., Huang, W.-N., Jean, J.-H., & Wu, W. (1991) *J. Biol. Chem. 266*, 3252−3259.
Chien, K.-Y., Chiang, C.-M., Hseu, Y.-C., Vyas, A. A., Rule, G. S., & Wu, W. (1994) *J. Biol. Chem. 269*, 14473−14483.
Creighton, T. E. (1993) in *Proteins: structures and molecular properties*, W. H. Freeman and Co., New York.
Cutler, R. L., Davies, A. M., Creighton, S., Warshel, A., Moore, G. R., et al. (1989) *Biochemistry 28*, 3188−3197.
Dauplais, M., Neumann, J. M., Pinkasfeld, S., Ménez, A., & Roumestand, C. (1995) *Eur. J. Biochem. 230*, 213−220.
Dufton, M. J., & Hider, R. C. (1991) in *Snake venom* (Harvey, A. L., Ed.) pp 259−302, Pergamon Press, New York.
Dyson, H. J., Merutka, G., Waltho, J. P., Lerner, R. A., & Wright, P. E. (1992a) *J. Mol. Biol. 226*, 795−817.
Dyson, H. J., Sayre, J. R., Merutka, G., Shin, H.-C., Lerner, R. A., & Wright, P. E. (1992b) *J. Mol. Biol. 226*, 819−835.
Ebina, S., & Wüthrich, K. (1984) *J. Mol. Biol. 179*, 283−288.
Ellman, G. L. (1959) *Arch. Biochem. Biophys. 82*, 70−73.
Fan, P., Bracken, C., & Baum, J. (1993) *Biochemistry 32*, 1573−1582.
Forman-Kay, J. D., Clore, G. M., & Gronenborn, A. M. (1992) *Biochemistry 31*, 3442−3452.
Galat, A., Yang, C. C., & Blout, E. R. (1985) *Biochemistry 24*, 5678−5685.
Gilquin, B., Roumestand, C., Zinn-Justin, S., Ménez, A., & Toma, F. (1993) *Biopolymers 33*, 1659−1675.
Greenfield, N., & Fasman, G. D. (1969) *Biochemistry 8*, 4108−4116.
Hseu, Y.-C., & Wu. W. (1995) *FASEB J. 9*, A1371.
Jahnke, W., Mierke, D. F., Beress, L., & Kessler, H. (1994) *J. Mol. Biol. 240*, 445−458.
Jeener, J., Meier, B. H., Bachman, P., & Ernst, R. R. (1979) *J. Chem. Phys. 71*, 4546−4553.
Jeng, M.-F., & Dyson, H. J. (1996) *Biochemistry 35*, 1−6.
Kohda, D., Sawada, T., & Inagaki, F. (1991) *Biochemistry 30*, 4869−4900.
Lauterwein, J., Lazdunski, M., & Wüthrich, K. (1978) *Eur. J. Biochem. 92*, 361−371.
Llinás, M., & Klein, M. P. (1975) *J. Am. Chem. Soc. 97*, 4731−4737.
Low, B., & Corfield, P. W. R. (1986) *Eur. J. Biochem. 161*, 579−587.
Macquaire, F., Baleux, F., Giaccobi, E., Huynh-Dinh, T., Neuman, J.-M., & Sanson, A. (1992) *Biochemistry 31*, 2576−2582.
Macura, S., & Ernst, R. R. (1980) *Mol. Phys. 41*, 95−117.

Marion, D., & Wüthrich, K. (1983) *Biochem. Biophys. Res. Commun. 113*, 967−974.
Nelson, J. W., & Kallenbach, N. R. (1986) *Proteins: Struct., Funct., Genet. 1*, 211−217.
O'Connell, J. F., Bougis, P. E., & Wüthrich, K. (1993) *Eur. J. Biochem. 213*, 891−900.
Otting, G., Steinmetz, W. E., Bougis, P. E., Rochat, H., & Wüthrich, K. (1987) *Eur. J. Biochem. 168*, 609−620.
Pardi, A., Wagner, G., & Wüthrich, K. (1983) *Eur. J. Biochem. 137*, 445−454.
Piotto, M., Saudek, V., & Sklenár, V. (1992) *J. Biomol. NMR 2*, 661−665.
Rees, B., Bilwes, A., Samama, J. P., & Moras, D. (1990) *J. Mol. Biol. 214*, 281−297.
Riddles, P. W., Blakele, R. L., & Zerner, B. (1983) *Methods Enzymol. 91*, 49−60.
Rizo, J., Blanco, F. J., Kobe, B., Bruch, M. D., & Gierasch, L. M. (1993) *Biochemistry 32*, 4881−4894.
Roumestand, C., Gilquin, B., Tremeau, O., Gatineau, E., Mouawad, L., Ménez, A., & Toma, F. (1994) *J. Mol. Biol. 243*, 719−735.
Scott, D. L., Mandel, A. M., Sigler, P. B., & Honig, B. (1994) *Biophys. J. 67*, 493−504.
Segawa, S.-I., Fukuno, T., Fujiwara, K., & Noda, Y. (1991) *Biopolymers 31*, 497−509.
Serrano, L. S., Horovitz, A., Avron, B., Bycroft, M., & Fersht, A. R. (1990) *Biochemistry 29*, 9343−9352.
Shiraki, K., Nishikawa, K., & Goto, Y. (1995) *J. Mol. Biol. 245*, 180−194.
Singhal, A. K., Chien, K.-Y., Wu, W., & Rule, G. S. (1993) *Biochemistry 32*, 8036−8044.
Sönnichsen, F. D., Van Eyk, J. E., Hodges, R. S., & Sykes, B. D. (1992) *Biochemistry 32*, 6348−6355.
Steinmetz, W. E., Moonen, C., Kumar, A., Lazdunski, M., Visser, L., Carlsson, F. H. H., & Wüthrich, K. (1981) *Eur. J. Biochem. 120*, 467−475.
Steinmetz, W. E., Bougis, P. E., Rochat, H., Redwine, O. D., Braun, W., & Wüthrich, K. (1988) *Eur. J. Biochem. 172*, 101−116.
Sun, Y.-J., Wu, W., Chiang, C.-M., Hsin, A.-Y., & Hsiao, C.-D. (1996) submitted to *J. Biol. Chem*.
Surewicz, W. K., Stepanik, T. M., Szabo, A. G., & Mantsch, H. H. (1988) *J. Biol. Chem. 263*, 786−790.
Thomas, P. D., & Dill, K. A. (1993) *Protein Sci. 2*, 2050−2065.
Warshel, A., & Aqvist, J. (1991) *Annu. Rev. Biophys. Chem. 20*, 267−298.
Williams, R. J. P. (1989) *Eur. J. Biochem. 183*, 479−497.
Wishart, D. S., Sykes, B. D., & Richards, F. M. (1992) *Biochemistry 31*, 1647−1651.
Wüthrich, K. (1986) *NMR of proteins and nucleic acids*, Wiley-Interscience, New York.
Yu, C., Lee, C.-S., Chuang, L.-C., Shei, Y.-R., & Wang, C. Y. (1990) *Eur. J. Biochem. 193*, 789−799.
Yu, C., Bhaskaran, R., Chuang, L.-C., & Yang, C. C. (1993) *Biochemistry 32*, 2131−2138.
Zhong, L., & Johnson, W. C. (1992) *Proc. Natl. Acad. Sci. U.S.A. 89*, 4462−4465.

BI960077T